Supplement on RC

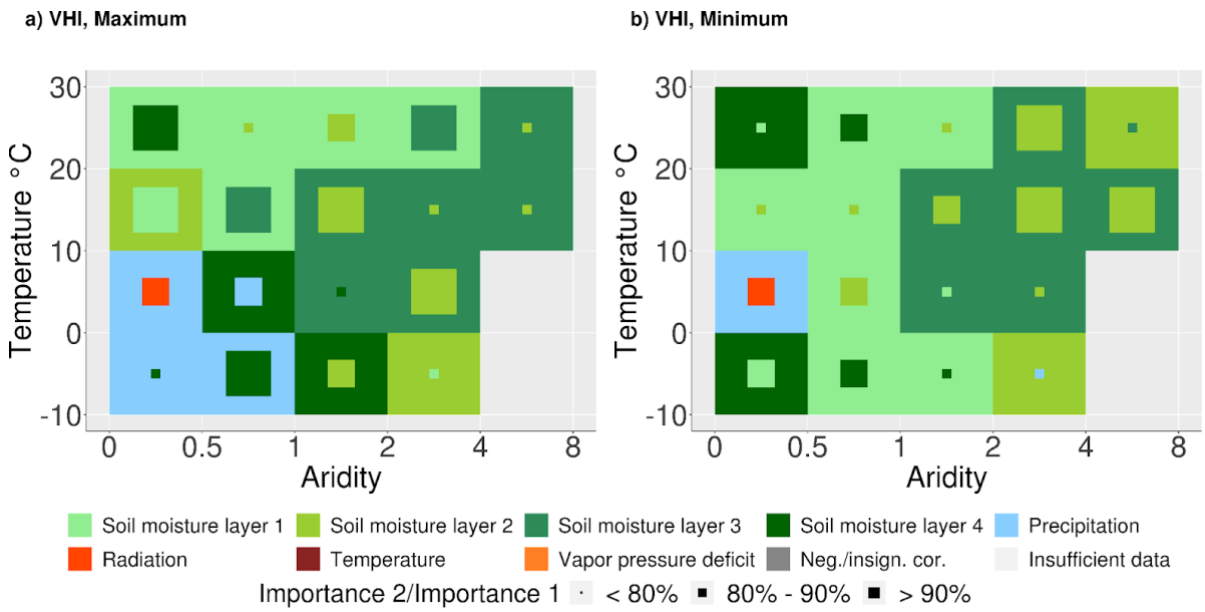

Figure 1*: Hydrometeorological controls (ERA5 land) of different climate regimes on VHI from NOAA (Kogan et al., 1995). Grid cells are grouped by their long-term temperature and aridity (unit-adjusted net radiation/precipitation). The variable which is important for most of the grid cells for vegetation productivity maxima (a) and minima b), inferred using ET, in one climate regime is used to color the box. The second most important variable colors the smaller squares. Their ratio is denoted in the size of the squares.

Main manuscript figures

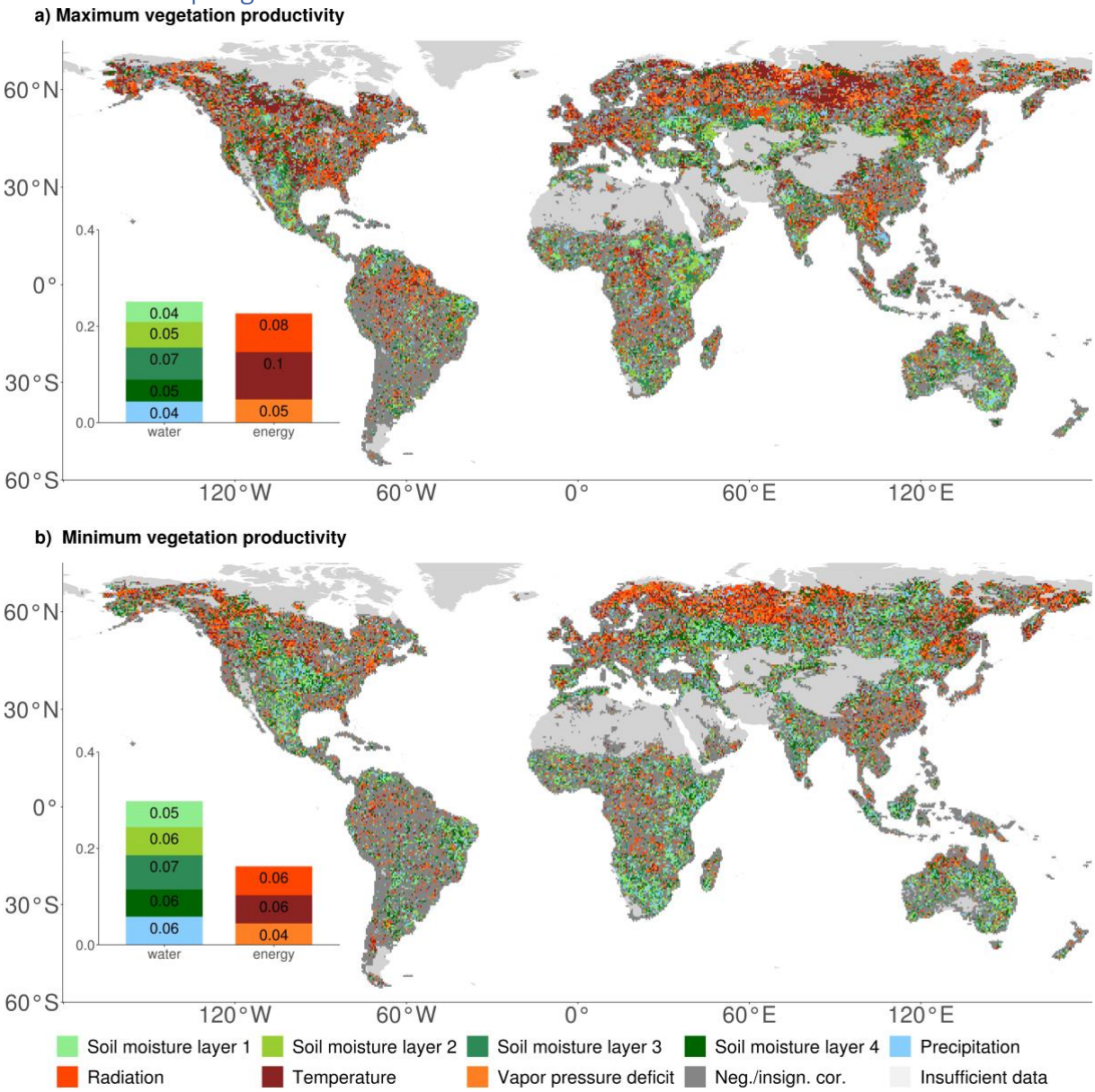

Figure 4. Global distribution of hydrometeorological controls of Sun-Induced Fluorescence (SIF) (a) maxima and (b) minima in respective colors, as assessed from strongest correlations. The inset bar plot indicates the area controlled by each variable relative to the total study area. Dark grey color denotes the study area, in which correlations are negative/insignificant.

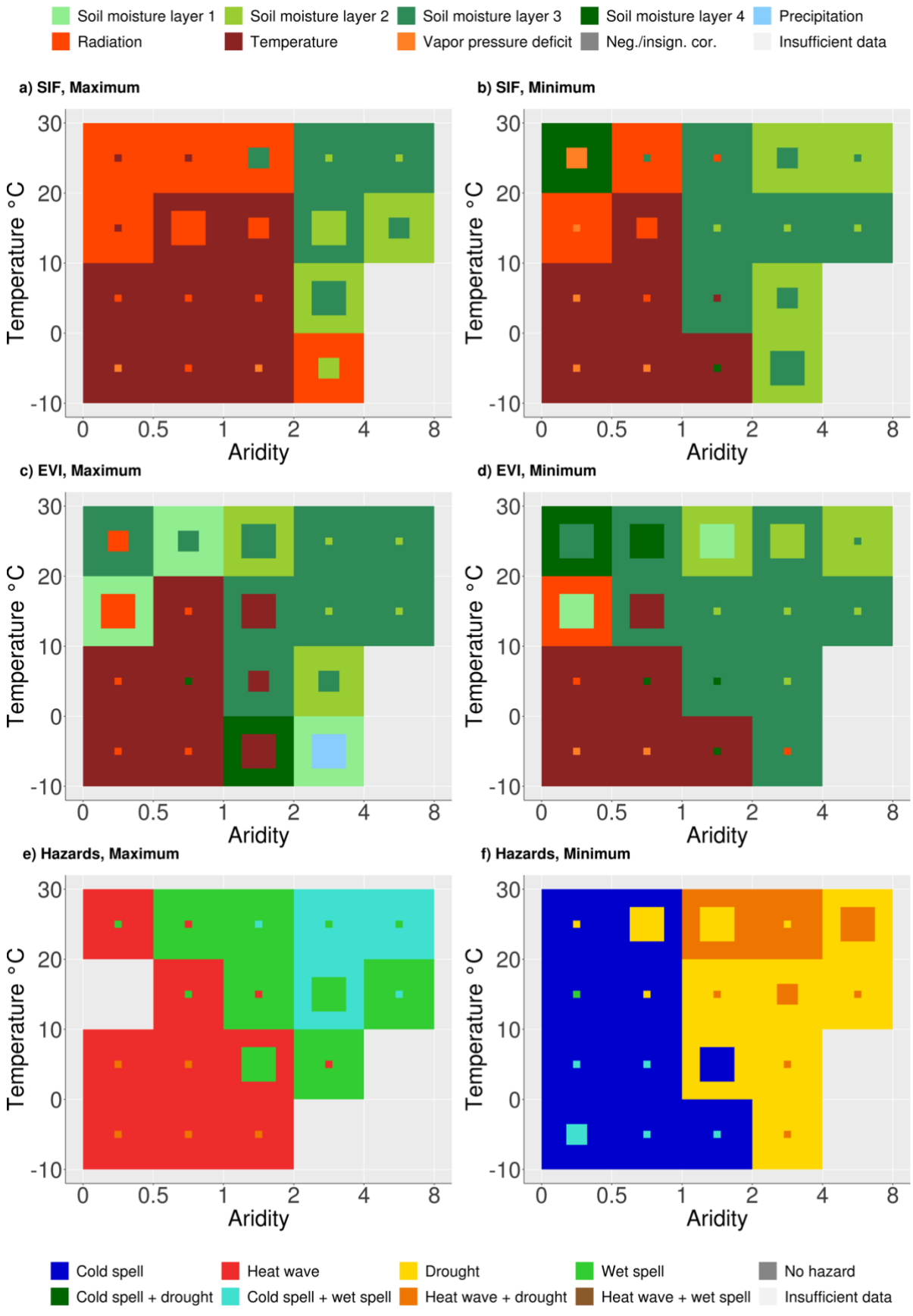
Soil moisture layer 1
Soil moisture layer 2
Soil moisture layer 3
Soil moisture layer 4
Precipitation
Radiation
Temperature
Vapor pressure deficit
Neg./insign. cor.
Insufficient data
a) SIF, Maximum
b) SIF, Minimum
c) EVI, Maximum
d) EVI, Minimum
e) Hazards, Maximum
f) Hazards, Minimum
Temperature °C
Aridity
30
20
10
0
-10
0
0.5
1
2
4
8
Cold spell
Heat wave
Drought
Wet spell
No hazard
Cold spell + drought
Cold spell + wet spell
Heat wave + drought
Heat wave + wet spell
Insufficient data
Importance 2/Importance 1
< 80%
80% - 90%
> 90%

Figure 5. Hydrometeorological controls of vegetation productivity extremes summarized across climate regimes, (a) and (b) for Sun-Induced Fluorescence (SIF) extremes, (c) and (d) for Enhanced Vegetation Index (EVI) extremes. (e) and (f) display the hydrometeorological hazards co-occurring with the SIF extremes. Box color denotes the main controlling hydrometeorological variable, the second most important variable is indicated in the smaller squares' color, while its size represents the ratio between highest/second highest amounts of grid cells.

Supplementary material figures

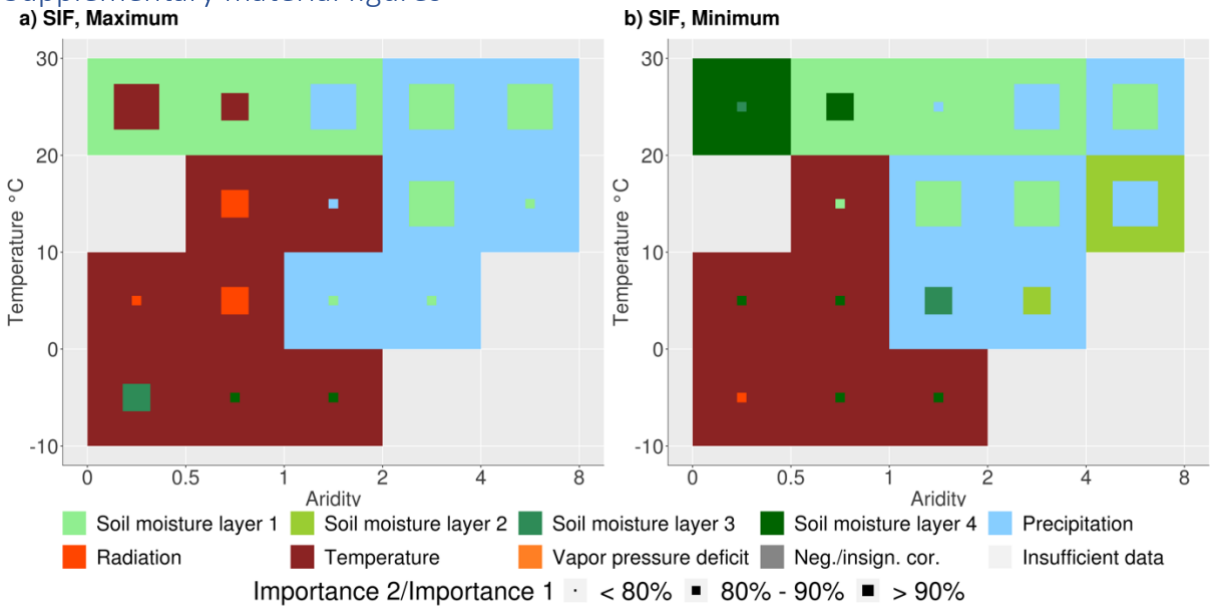

Fig. S4. Hydrometeorological controls (ERA5 land) of different climate regimes with a lag time of 1 month. Grid cells are grouped by their long-term temperature and aridity (unit-adjusted net radiation/precipitation). The hydrometeorological variables of the month preceding the SIF extreme have been used in the computation of most important variable. The variable which is important for most of the grid cells for vegetation productivity maxima (a) and minima b), inferred using SIF, in one climate regime is used to color the box. The second most important variable colors the smaller squares. Their ratio is denoted in the size of the squares.

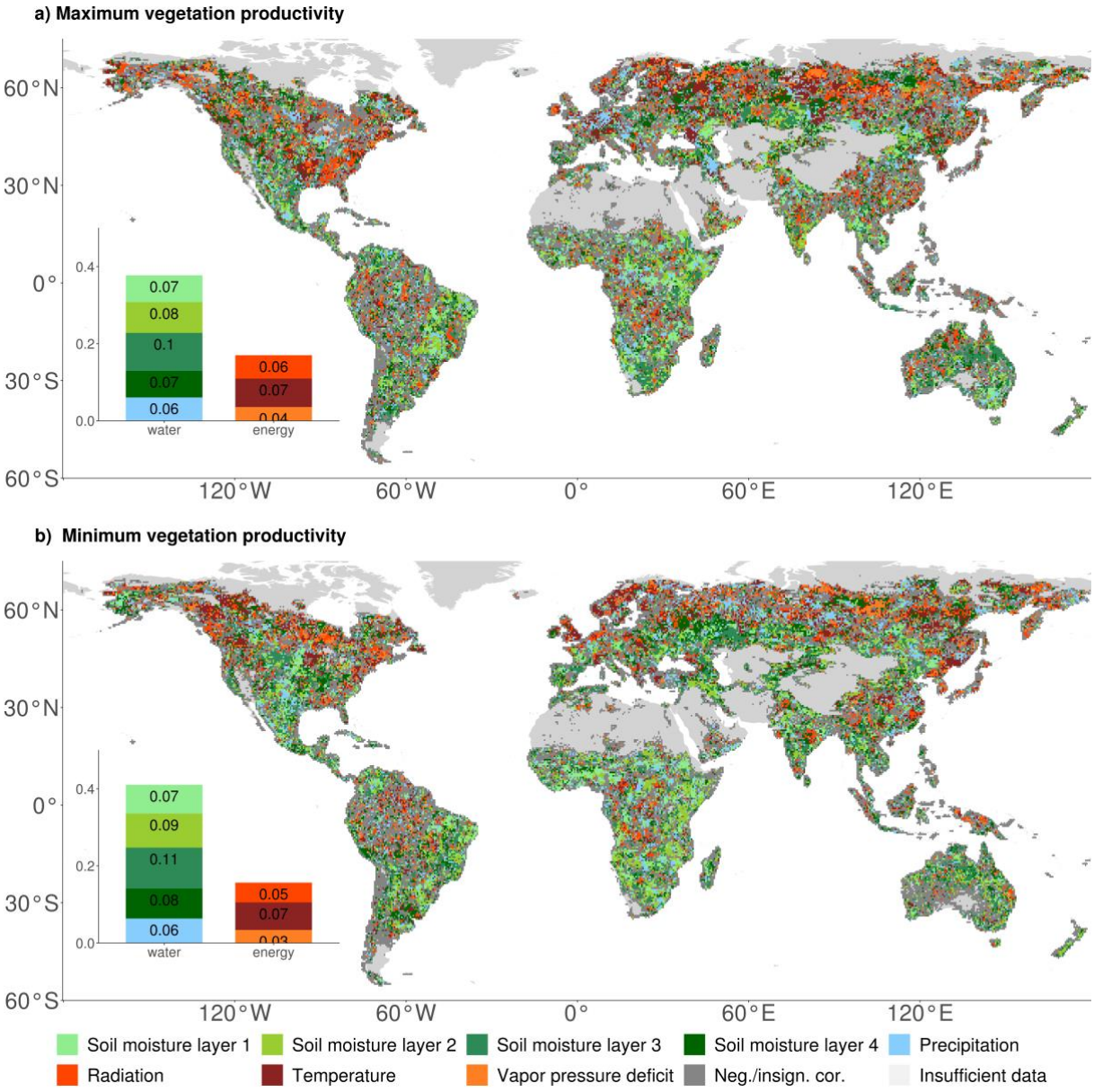

Fig. S5. Global distribution of hydrometeorological controls (ERA5 land) of EVI (a) maxima and (b) minima. The displayed variable correlates strongest with EVI in the extreme months, considering only significant and positive correlations. The bar plot indicates the area controlled by each variable relative to the total study area.

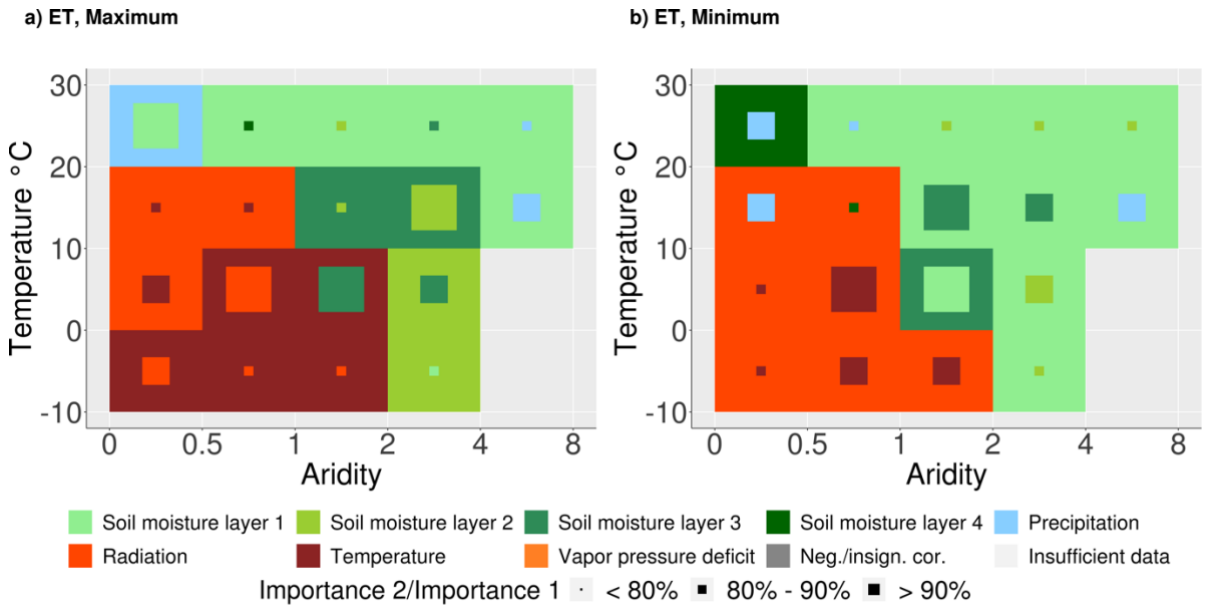

Fig. S6. Hydrometeorological controls (ERA5 land) of different climate regimes on ET from GLEAM. Grid cells are grouped by their long-term temperature and aridity (unit-adjusted net radiation/precipitation). The variable which is important for most of the grid cells for vegetation productivity maxima (a) and minima b), inferred using ET, in one climate regime is used to color the box. The second most important variable colors the smaller squares. Their ratio is denoted in the size of the squares.

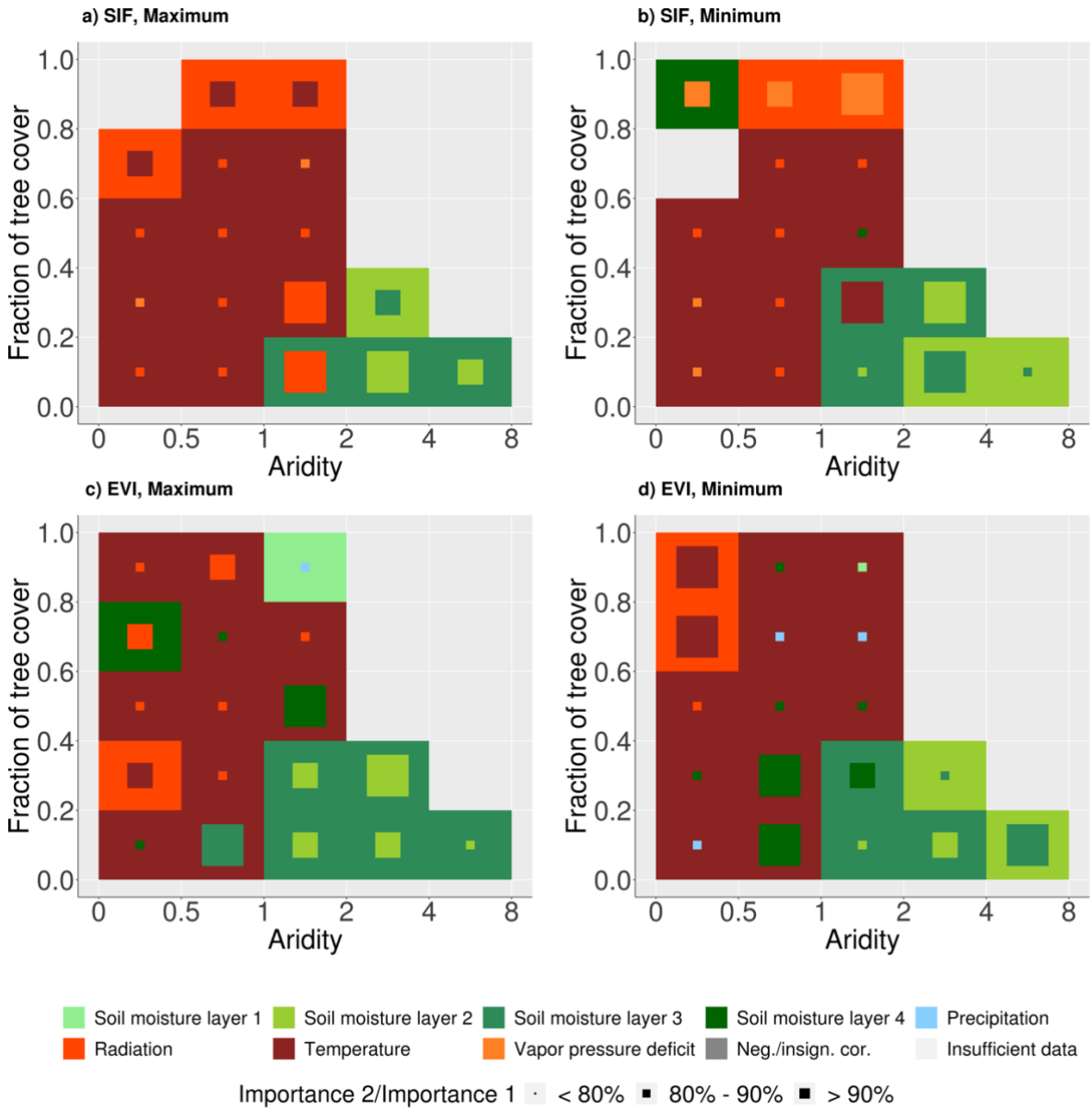

Fig. S7. Hydrometeorological controls (ERA5 land) of different vegetation regimes. Grid cells are grouped by their fraction of tree cover and aridity (unit-adjusted net radiation/precipitation). The variable which is important for most of the grid cells for vegetation productivity extremes (a) and b) SIF; c) and d) EVI) in one vegetation regime is used to color the box. The second most important variable colors the smaller squares. Their ratio is denoted in the size of the squares.

References

Joiner, J., Guanter, L., Lindstrot, R., Voigt, M., Vasilkov, A. P., Middleton, E. M., ... & Frankenberg, C. (2013). Global monitoring of terrestrial chlorophyll fluorescence from moderate-spectral-resolution near-infrared satellite measurements: methodology, simulations, and application to GOME-2. Atmospheric Measurement Techniques, 6(10), 2803-2823. https://doi.org/10.5194/amt-6-2803-2013

Jonard, F., De Cannière, S., Brüggemann, N., Gentine, P., Short Gianotti, D. J., Lobet, G., Miralles, D. G., Montzka, C., Pagán, B. R., Rascher, U., & Vereecken, H. (2020). Value of sun-induced chlorophyll fluorescence for quantifying hydrological states and fluxes: Current status and challenges. Agricultural and Forest Meteorology, 291(June), 108088. https://doi.org/10.1016/j.agrformet.2020.108088

Karnieli, A., Bayasgalan, M., Bayarjargal, Y., Agam, N., Khudulmur, S., & Tucker, C. J. (2006). Comments on the use of the vegetation health index over Mongolia. International Journal of Remote Sensing, 27(10), 2017-2024. https://doi.org/10.1080/01431160500121727

Kogan, F. N. (1995). Application of vegetation index and brightness temperature for drought detection. Adv. Sp. Res. 15, 91–100. https://doi.org/10.1016/0273-1177(95)00079-T

Köhler, P., Frankenberg, C., Magney, T. S., Guanter, L., Joiner, J., & Landgraf, J. (2018). Global retrievals of solar-induced chlorophyll fluorescence with TROPOMI: First results and intersensor comparison to OCO-2. Geophysical Research Letters, 45(19), 10-456. https://doi.org/10.1029/2018GL079031

Sun, Y., Fu, R., Dickinson, R., Joiner, J., Frankenberg, C., Gu, L., Xia, Y., & Fernando, N. (2015). Drought onset mechanisms revealed by satellite solar-induced chlorophyll fluorescence: Insights from two contrasting extreme events. Journal of Geophysical Research G: Biogeosciences, 120(11), 2427–2440. https://doi.org/10.1002/2015JG003150

Turner, A. J., Köhler, P., Magney, T. S., Frankenberg, C., Fung, I., and Cohen, R. C. (2020). A double peak in the seasonality of California's photosynthesis as observed from space, Biogeosciences, 17, 405–422, https://doi.org/10.5194/bg-17-405-2020.

Veefkind, J. P., Aben, I., McMullan, K., Förster, H., De Vries, J., Otter, G., ... & Levelt, P. F. (2012). TROPOMI on the ESA Sentinel-5 Precursor: A GMES mission for global observations of the atmospheric composition for climate, air quality and ozone layer applications. Remote sensing of environment, 120, 70-83. https://doi.org/10.1016/j.rse.2011.09.027

Zhou, S., Zhang, Y., Williams, A. P., & Gentine, P. (2019). Projected increases in intensity, frequency, and terrestrial carbon costs of compound drought and aridity events. Science advances, 5(1), eaau5740. https://doi.org/10.1126/sciadv.aau5740